Narrow-band microcavity waveguides in photonic crystals

Amir Boag and Ben Zion Steinberg

Faculty of Engineering, Tel Aviv University, Tel Aviv 69978, Israel

Received October 10, 2000; revised manuscript received February 26, 2001; accepted March 28, 2001

A novel device, formed by a widely spaced periodic array of defects in a photonic bandgap crystal, is studied with the goal of designing a waveguide with a prescribed narrow bandwidth. Tunneling of radiation between the defect sites allows wave propagation along the line of the defects. An analytical study based on the weakly coupled cavity model is performed, and the dispersion relation $\omega(\beta)$ of the new waveguide is derived. The frequency shift and the band structure of the periodic defect waveguide are linked by an analytic relationship to the distance between the defect sites and therefore can be tuned by varying the latter. Sections of such waveguides can be employed as ultra-narrow-band filters in optical routing devices. Numerical simulations demonstrate the performances of this new device and support the analytical predictions. © 2001 Optical Society of America

OCIS code: 130.2790.

1. INTRODUCTION

Photonic bandgap materials have attracted much attention in the context of designing optical and microwave devices. Studies have shown that local defects in photonic crystals can be used to create localized electromagnetic fields within the frequency gap of the unperturbed photonic crystals. The localized mode frequency depends on the exact nature of the local defect.[1,2] Numerical experiments have shown that a line of a repeated defect in photonic crystals can be used to guide optical signals,[1] to create frequency-selective waveguides by properly designing the nature of the repeated defect,[3] and also to multiplex and demultiplex these signals.[4] Most researchers studying wave guiding by line defects employ photonic band waveguides obtained by removal or modification of consecutive nearby posts in the periodic structure. The strong coupling between the adjacent defects produces relatively wideband waveguides. Coupling between two microcavities that are formed by two local defects separated by a distance larger than the basic photonic crystal period size (widely spaced defects) was studied in Ref. 5. However, the interest there was essentially in the generation and shift of additional line spectra, and the propagation of electromagnetic radiation along a line of such separated defects was not addressed.

In this paper we extend and elaborate on the preliminary investigation reported previously in Ref. 6. Here we address the issue of designing photonic bandgap waveguides with a prescribed narrow bandwidth. Specifically, we concentrate on the problem of a waveguide formed by *widely spaced* periodic defects in the photonic bandgap crystal. Tunneling of radiation between the defect sites allows wave propagation along the line of defects. Sections of such waveguides can be employed as ultra-narrow-band filters in optical routing devices. Here we propose an asymptotic analytical study and exact numerical simulation of these devices. The analytical study is based on the weakly coupled cavity model. This approach resembles the tight binding perturbation theory of solid-state physics.[7] (A similar analytical approach has been applied in the context of photonic crystals with application to field enhancement and nonlinear optics.[8]) A single defect mode with a resonant frequency ω_0 in the bandgap is introduced first. Coupling between the periodic defects causes the discrete spectral line at ω_0 to turn into a narrow band of guided frequencies slightly shifted from the original frequency ω_0 of the single defect. Perturbation theory facilitates an approximate calculation of both the frequency shift and the band structure of the periodic defect waveguide. Furthermore, these parameters are linked by an analytic relationship to the distance between the defect sites. Consequently, the latter distance can be directly adjusted to achieve the desirable waveguide properties.

The validity of our analytical results is verified by a comparison with numerically rigorous computations. Here, care must be taken to handle the new configuration properly. Since the perfect multidimensional periodicity of the background photonic crystal no longer exists in the presence of the periodic array waveguide, and since weak coupling among remote microcavities constitutes the basic physics of the device under study, numerical approaches that assume perfect multidimensional periodicity and/or suffer from unwanted coupling artifacts such as the plane wave and supercell methods[1,2] are ruled out altogether. Furthermore, we wish to check the performance of the new devices in a realistic configuration in which finite-size specimens are used. Thus, from the numerical point of view, we formulate the problem as that of fully vectorial scattering in which the scatterer is a dielectric body of arbitrary shape that assumes no periodicity at all. A well-tested and efficient approach for solving such scattering problems is the current model technique reported, for example, in Refs. 9 and 10. To reduce the complexity of the problem, the numerical simulations are performed for two-dimensional crystals, although the

0740-3232/2001/112799-07$15.00

analytical study is valid for both two- and three-dimensional geometries. The results of numerical computations support the analytical predictions.

2. DESCRIPTION OF THE PROBLEM AND FORMULATION

Our analysis here applies to two-dimensional and three-dimensional photonic crystals. For clarity, the basic configuration under study is schematized in two dimensions in Fig. 1. A photonic crystal with primitive lattice vectors a_1, a_2, and a_3 (the smallest vectors pointing from one lattice point to another) is characterized by a periodic relative permittivity $\epsilon_p(r)$, as shown in Fig. 1(a). A single local defect of arbitrary nature is shown schematically in Fig. 1(b). We term this defect the basic microcavity. The relative permittivity of the photonic crystal in the presence of the basic microcavity is denoted by $\epsilon_d(r)$. We define the difference in the reciprocal relative permittivities between the microcavity-perturbed and unperturbed crystals by $d(r)$:

$$d(r) \equiv \frac{1}{\epsilon_d(r)} - \frac{1}{\epsilon_p(r)}. \tag{2.1}$$

This quantity is different from zero only near the basic microcavity. It will be used below in subsequent derivations. A linear array of identical defects can be formed now by periodic repetitions of the basic microcavity, as shown in Figs. 1(c) and 1(d). The intercavity vector, defined as the vector connecting two consecutive microcavities in the array, is denoted by b. Since the repeated microcavity locations are restricted to the photonic crystal points, we must have

$$b = \sum_{i=1}^{3} m_i a_i, \tag{2.2}$$

where $\{a_i\}_{i=1,\ldots 3}$ is the set of primitive lattice vectors and $\{m_i\}_{i=1,\ldots 3}$ is a set of constant integers that quantify the distance between two adjacent microcavities in units of basic lattice cells. The reciprocal relative permittivity of the photonic crystal with the linear array can be written now as

$$\frac{1}{\epsilon(r)} = \frac{1}{\epsilon_p(r)} + \sum_{n=-\infty}^{\infty} d(r - nb), \tag{2.3}$$

where $d(r)$ is defined in Eq. (2.1).

Our purpose is to study the propagation of time-harmonic electromagnetic waves in this configuration. The time-harmonic electromagnetic problem in an inhomogeneous dielectric can be cast in an eigenvalue form for the vector magnetic field H (Ref. 1):

$$\Theta H(r) = \left(\frac{\omega}{c}\right)^2 H(r), \tag{2.4}$$

where ω is the frequency, c is the free-space speed of light, and Θ denotes a Hermitian operator defined by

$$\Theta H \equiv \nabla \times \left[\frac{1}{\epsilon(r)} \nabla \times H\right]. \tag{2.4a}$$

Alternatively, the eigenfrequencies can be expressed in the variational form[1]

$$\left(\frac{\omega}{c}\right)^2 = \frac{\langle H, \Theta H\rangle}{\langle H, H\rangle}, \tag{2.5}$$

where $\langle \cdot, \cdot \rangle$ denotes the inner product defined by

$$\langle F, G\rangle = \int F \cdot \bar{G} \mathrm{d}r \tag{2.6}$$

and $F \cdot \bar{G}$ is the Cartesian scalar product of the two three-dimensional vector fields F and G and the overbar denotes a complex conjugate.

It is well known that often a local defect in a photonic crystal allows for a localized "trapped" mode with a frequency falling in the bandgap of the unperturbed crystal.[1] Thus we denote the magnetic field of the localized mode associated with the basic microcavity and the corresponding frequency by $H_0(r)$ and ω_0, respectively. By analogy to Eq. (2.4), the localized mode satisfies the equation

$$(\Theta^{\mathrm{per}} + \Theta_0) H_0(r) = \left(\frac{\omega_0}{c}\right)^2 H_0(r), \tag{2.7}$$

where Θ^{per} is the operator of the periodic structure and Θ_0 is the defect operator. We define the operators Θ^{per} and Θ_0 by analogy to Eq. (2.4a) by replacing $1/\epsilon(r)$ with $1/\epsilon_p(r)$ and with $d(r)$ [see Eq. (2.1)], respectively. Since Θ^{per} and Θ_0 are self-adjoint real operators, it is easily verified that for a lossless medium we can normalize $H_0(r)$ such that

$$\mathrm{Im}[H_0(r)] = 0. \tag{2.7a}$$

Now we turn to the case of the linear array obtained by periodic repetition of the basic microcavity. The reciprocal relative permittivity of the entire structure is given in Eq. (2.3). The operator Θ, which corresponds to the photonic crystal *with* the linear array of defects, can be written now as

$$\Theta = \Theta^{\mathrm{per}} + \sum_{n=-\infty}^{\infty} \Theta_n, \tag{2.8}$$

which comprises a superposition of Θ^{per} and shifted operators Θ_n defined by analogy with Eq. (2.4a) by replacement of $1/\epsilon(r)$ with $d(r - nb)$ for $n \in \mathbb{Z}$. Two observations are made now: First, the basic microcavity mode is well confined around the local defect. Second, if the basic microcavities are widely spaced, their mutual coupling is weak and the local field is well approximated by the field of a single isolated microcavity. Thus we follow the strong binding perturbation theory[7] and describe the modal solution of the entire problem as a summation over appropriately shifted versions of the basic microcavity mode:

$$H(r) = \sum_{n=-\infty}^{\infty} A_n H_n(r), \qquad H_n(r) \equiv H_0(r - nb), \tag{2.9}$$

where $\{A_n\}_{n\in\mathbb{Z}}$ is a set of yet-to-be-determined coefficients. Substitution of Eq. (2.9) into Eq. (2.5) yields

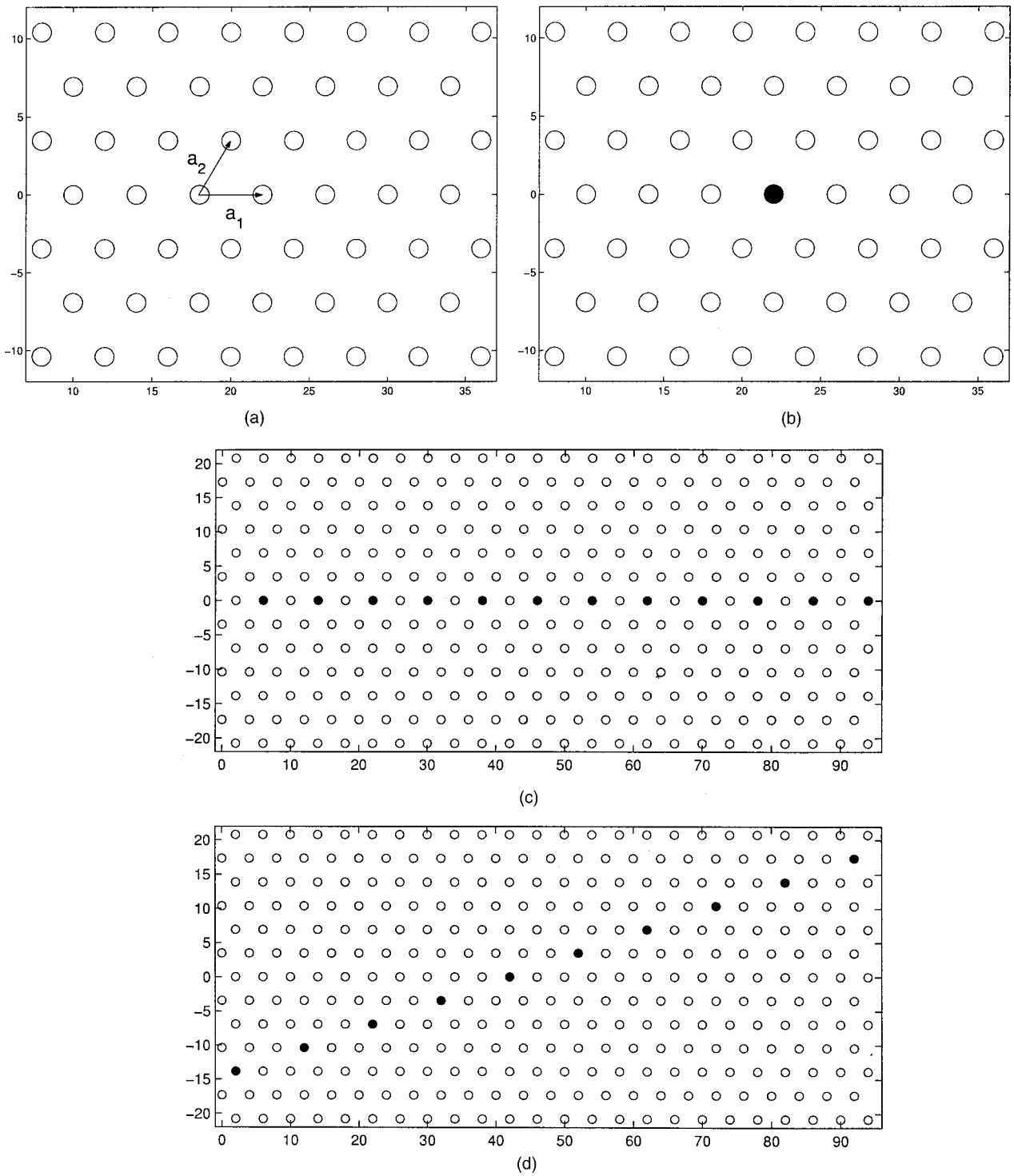

Fig. 1. Elements of the microcavity array waveguide. (a) Unperturbed background photonic crystal, with periodic relative permittivity $\epsilon_p(r)$. (b) Basic microcavity, created by a local defect of arbitrary nature. The relative permittivity of the crystal with the basic microcavity is $\epsilon_d(r)$. (c) Linear array formed by periodic repetitions of the basic microcavity by use of an intercavity vector $b = 2a_1$. (d) Same as (c) but with an intercavity vector $b = 2a_1 + a_2$.

$$\left(\frac{\omega}{c}\right)^2 = \frac{\sum_{n=-\infty}^{\infty}\sum_{m=-\infty}^{\infty} A_n \bar{A}_m \langle H_n, \Theta H_m\rangle}{\sum_{n=-\infty}^{\infty}\sum_{m=-\infty}^{\infty} A_n \bar{A}_m \langle H_n, H_m\rangle}. \tag{2.10}$$

Since the array is periodic and since Θ is self-adjoint, the inner products in Eq. (2.10) depend only on the difference $n - m$, and this dependence is Hermitian. Thus we define

$$h_{n-m} \equiv \langle H_n, H_m\rangle = \bar{h}_{m-n}, \tag{2.11a}$$

$$t_{n-m} \equiv \langle H_n, \Theta H_m\rangle = \bar{t}_{m-n}. \tag{2.11b}$$

Furthermore, using Eqs. (2.7) and (2.8), we can write a relation between t_m and h_m:

$$t_m = \left(\frac{\omega_0}{c}\right)^2 h_m + \sum_{n=-\infty, n\neq 0}^{\infty} t'_{mn}, \tag{2.12}$$

where

$$t'_{mn} \equiv \langle H_m, \Theta_n H_0 \rangle, \qquad \mathrm{Im}[t'_{mn}] = 0 \tag{2.12a}$$

and where the realness of t'_{mn} follows from that of H_0 [see Eq. (2.7a)]. According to the variational principle in Eq. (2.5), the frequency expressed in Eq. (2.10) is stationary (extremal point) with respect to the coefficients $\{A_n\}$. Therefore

$$\forall k, \quad \frac{\partial}{\partial A_k}\left(\frac{\omega}{c}\right)^2 = 0 \Rightarrow \sum_{m=-\infty}^{\infty}\left[t_{k-m} - \left(\frac{\omega}{c}\right)^2 h_{k-m}\right]\bar{A}_m = 0, \tag{2.13a}$$

$$\forall k, \quad \frac{\partial}{\partial \bar{A}_k}\left(\frac{\omega}{c}\right)^2 = 0 \Rightarrow \sum_{n=-\infty}^{\infty}\left[t_{n-k} - \left(\frac{\omega}{c}\right)^2 h_{n-k}\right]A_n = 0, \tag{2.13b}$$

and, because of the hermiticity of h_n and t_n [see Eqs. (2.11a) and (2.11b)], relations (2.13a) and (2.13b) are equivalent. Thus we have

$$\sum_{m=-\infty}^{\infty}\left[t_m - \left(\frac{\omega}{c}\right)^2 h_m\right]A_{m+k} = 0 \quad \forall k. \tag{2.14}$$

The form of Eq. (2.14) is shift invariant with respect to k. This implies a modal solution for A_m:

$$A_m = \exp(i\beta m), \tag{2.15}$$

where β is the (yet-to-be-determined) wave number associated with modal propagation in the linear array waveguide. Substituting Eq. (2.15) into Eq. (2.14) and using Eq. (2.12), we get

$$\left(\frac{\omega}{c}\right)^2 - \left(\frac{\omega_0}{c}\right)^2 = \frac{\sum_m \sum_{n\neq 0} t'_{mn}\exp(i\beta m)}{\sum_m h_m \exp(i\beta m)}, \tag{2.16}$$

where t'_{mn} is defined in Eq. (2.12a). Equation (2.16) is an expression for the frequency shift of the linear array mode with wave number $\beta/|b|$ relative to the frequency of the localized mode. For sufficiently spaced defects, we can make the first-order approximation by retaining only the nearest-neighbor interactions. This procedure is examined in Subsection 2.A.

A. Dominant Terms in Eq. (2.16) and Approximate Bandwidth

It can be seen from Eq. (2.11a) that h_m is the inner product of two basic microcavity modes $[H_m = H_0(r - mb)]$ separated a distance $mb = m\,\Sigma_i m_i a_i$. Since defect modes decay exponentially away from the defect,[1] this inner product decreases very rapidly with increasing m. Thus the dominant term in the donominator of Eq. (2.16) is h_0, which is nothing but the square of the H_0 norm. Consequently, we are left with

$$\left(\frac{\omega}{c}\right)^2 - \left(\frac{\omega_0}{c}\right)^2 \approx \|H_0\|^{-2}\sum_{m=-\infty}^{\infty}\sum_{n\neq 0} t'_{mn}\exp(i\beta m). \tag{2.17}$$

The evaluation of the numerator's dominant terms is somewhat more involved. We start by rewriting the operation $\Theta_n H_0(r)$ as

$$\Theta_n H_0(r) = i\omega_0 \nabla \times [d(r - nb)\epsilon_d(r)E_0(r)], \tag{2.18}$$

where $E_0(r)$ is the electric field associated with the basic microcavity mode $H_0(r)$ and we make use of the fact that $\nabla \times H_0 = i\omega_0\epsilon_d(r)E_0(r)$. Substituting this result into Eq. (2.12a), using the standard vector identity $(\nabla \times A) \cdot B = \nabla \cdot (A \times B) + A \cdot (\nabla \times B)$, and applying the Gauss theorem, we find that

$$t'_{mn} = -i\omega_0 \int_{\partial V_n} d(r - nb)\epsilon_d(r) \times [\bar{E}_0(r) \times H_0(r - mb)] \cdot \mathrm{d}s + \omega_0^2 \int_{V_n} d(r - nb)\epsilon_d(r)\epsilon_d(r - mb) \times [\bar{E}_0(r) \cdot E_0(r - mb)]\mathrm{d}^3 r. \tag{2.19}$$

Recall that $d(r - nb)$ is different from zero only at the nth microcavity. Thus the integrations above are limited to the nth microcavity volume V_n and its surface ∂V_n. Since $E_0(r)$ and $H_0(r)$ become very small as r increases, and since the summation in relation (2.17) excludes the $n = 0$ term, the dominant terms are $(m, n) = (0, \pm 1)$ and $(m, n) = \pm(1, 1)$. Furthermore, for symmetric defects we have $t'_{01} = t'_{0-1}$ and $t'_{11} = t'_{-1-1}$. Thus

$$\left(\frac{\omega}{c}\right)^2 - \left(\frac{\omega_0}{c}\right)^2 \approx 2\|H_0\|^{-2}(t'_{01} + t'_{11}\cos\beta), \tag{2.20}$$

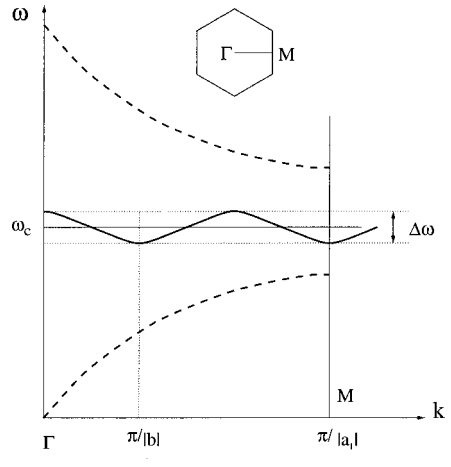

Fig. 2. Dispersion curve $\omega(\beta)$ of the microcavity array waveguide (solid curve). We assume here that $b = m_1 a_1$, with a_1 defined in Fig. 1(a) and $m_1 = 3$. The unperturbed crystal dispersion that corresponds to propagation along the vector a_1 (the wave numbers along Γ–M in the reciprocal lattice domain) is also shown (dashed curves).

where we have used the second equality in Eq. (2.12a). Relation (2.20) constitutes the dispersion relation $\omega(\beta)$ of the array waveguide. It can be seen that t'_{11} determines the total bandwidth of the array waveguide, whereas t'_{01} determines the central frequency shift relative to the basic microcavity frequency ω_0. Since E_0 and H_0 are well-localized fields that decay exponentially with the distance away from the microcavity, t'_{01} and t'_{11} decay exponentially as the intercavity vector b increases. Therefore, by tuning b, one can design extremely narrow-band waveguides. Invoking the narrow-band approximation $\omega^2 - \omega_0^2 \approx 2\omega_0(\omega - \omega_0)$, we further reduce relation (2.20) to

$$\omega - \omega_0 \approx \frac{c^2}{\omega_0 \|H_0\|^2}(t'_{01} + t'_{11}\cos\beta). \tag{2.21}$$

This dispersion relation is shown schematically in Fig. 2. Finally, note that, because of the mb and nb field shifts in Eq. (2.19), we have $|t'_{01}| \ll |t'_{11}|$, so the central frequency shift, relative to ω_0 and relative to the bandwidth, is negligible. Thus the waveguide central frequency $\omega_c = \omega_0 + c^2 t'_{01}/(\omega_0\|H_0\|^2)$ is approximately ω_0, and its relative bandwidth is given by

$$\frac{\Delta\omega}{\omega_0} = 2\left(\frac{c}{\omega_0\|H_0\|}\right)^2 t'_{11}. \tag{2.22}$$

Since $E_0(r)$ and $H_0(r)$ are localized fields that decay exponentially away from the defect site, it follows from Eq. (2.19) that this bandwidth decays exponentially with the increase of $|b|$.

3. NUMERICAL EXAMPLES

For the sake of simplicity, we study waveguides embedded in the two-dimensional photonic crystal previously investigated in Ref. 3. Specifically, we consider the problem of a free-standing finite periodic array of dielectric cylinders that is infinite in the z direction. The x, y-plane cross section of the problem geometry is illustrated in Fig. 1. The unperturbed hexagonal array is of the type shown in Fig. 1(a), with the intercylinder spacing $|a_1| = |a_2| = 4$ length units. The array comprises a total of 156 cylinders with centers confined within a rectangle $0 \leqslant x \leqslant 46$ and $|y| \leqslant 20.8$. All cylinders are 0.6 length unit radius and are characterized by a refractive index of 2.9. The specific locations of the cylinders are as depicted in Fig. 1(c), for $x < 47$. We assume TM polarization, i.e., a z-polarized electric field parallel to the cylinder axis. A basic microcavity is formed by removing a single cylinder, as shown in Fig. 1(b). The waveguiding structure is formed in the photonic crystal by the creation of defects along the line $y = 0$ by removing selected posts, using an intercavity vector $b = m_1 a_1$ [see Fig. 1(c)]. The center frequency of the resulting waveguide is determined mainly by the resonant frequency of a single defect resonance. The spacing between the defects determines the amount of coupling between the adjacent microcavities, which, according to the model presented in Section 2, strongly affects the bandwidth of the resulting waveguide. To demonstrate this effect by means of numerically rigorous computations, we have developed a program based on the current model technique.[9,10] In this technique the electromagnetic fields outside the cylinders and those in each cylinder are simulated by sets of currents of adjustable amplitudes. The amplitudes of the currents are determined by applying the boundary conditions, namely, the continuity of the tangential electric and magnetic fields on the surface of the cylinders. Since the boundary conditions are enforced in the point-matching sense, errors between the match points serve as a convenient measure of the accuracy of the numerical solution. To this end, we monitor the normalized rms boundary condition errors ΔE_{bc} and ΔH_{bc} for the electric and magnetic fields, as defined in Ref. 9.

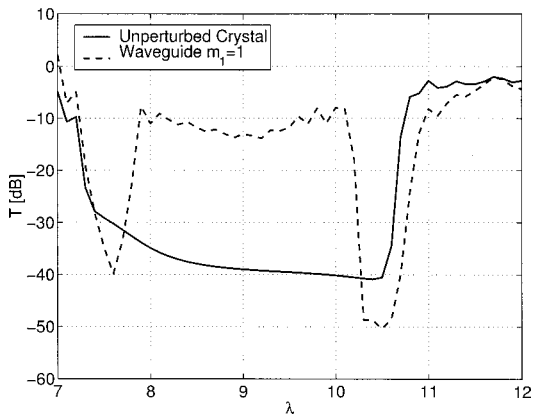

Fig. 3. Unperturbed crystal transmission curve and transmission of a waveguide obtained by removing a complete row of posts (dashed curve). The dashed curve corresponds to an array waveguide with intercavity vector $b = a_1$.

The attenuation of the waveguiding structure is evaluated by computing the ratio of the field intensity in the last cavity to that in the first one. The average squared electric field is computed across the first and the last microcavity along the segment $-5 \leqslant y \leqslant 5$ passing through the respective cavity center. Within the stop band, the ratio between these fields represents the decay of the field along the waveguide relatively independently of the mismatch between the waveguide and the free space. Reflections at the ends of the waveguide, however, are expected to produce a ripple of the field ratio in the passband. The cylinder array is illuminated by a plane wave propagating in the positive x direction. We surmise that a type of excitation (e.g., a plane wave or a Gaussian beam) does not affect the essential characteristics of the waveguiding structure.

First, to test the accuracy of the numerical computation, we evaluate the average electric field along the line $x = 48$, $-5 \leqslant y \leqslant 5$, for an unperturbed crystal that comprises all 156 cylinders. The boundary condition errors incurred in this computation are $\Delta E_{\mathrm{bc}} \approx 0.05\%$ and $\Delta H_{\mathrm{bc}} \approx 0.5\%$, which are sufficiently low to produce accurate results. The transmission of the unperturbed crystal, defined as the ratio between the average field specified above and the incident field, is plotted in Fig. 3 (solid curve). A clear bandgap is seen between the wavelengths $\lambda = 7.3$ and $\lambda = 10.7$. This bandgap is in good agreement with the results reported in Ref. 3. Next, we consider the "conventional" photonic crystal waveguide obtained by removing a horizontal row of posts. The corresponding transmission curve is also plotted in Fig. 3.

It can be seen that the transmission bandwidth is almost as large as the entire bandgap.

We turn now to study array waveguides formed by larger intercavity vectors. We start by characterizing the single defect mode. In all cases we use a microcavity created by removing a single post. The resonance of the single defect is at $\lambda_0 = 9.06$, and the corresponding mode is depicted in Fig. 4. Strong localization of the field about the center of the defect (the removed cylinder) justifies the application of the weak-coupling approximation when one is dealing with arrays of cavities. Finally, we study a number of waveguides with various spacings between these defects. Specifically, we perform calculations for three cases $b = a_1$ (all cylinders centered on line $y = 0$ are removed), $b = 2a_1$ [removing cylinders centered at $(x, y) = (6, 0)$, (14,0), (22,0), (30,0), (38,0), (46,0)], and $b = 3a_1$ [removing cylinders centered at $(x, y) = (10,0)$, (22,0), (34,0), (46,0)]. The structure of the field along the waveguides is presented in Fig. 5 for $b = 2a_1$ and $b = 3a_1$. Figure 5 clearly exemplifies the localized nature of the field at the defect sites. Also, one can see that the waveguide field can be represented by a superposition

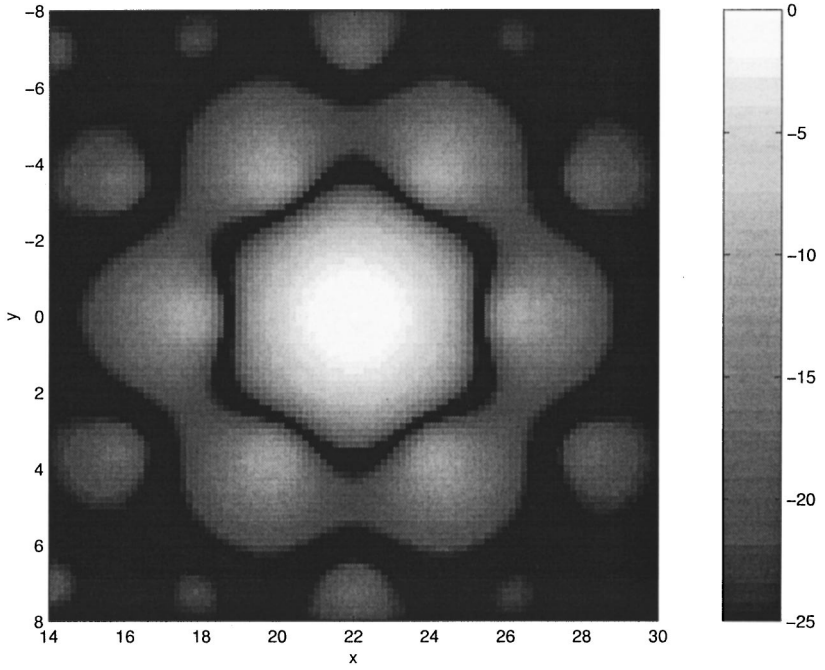

Fig. 4. Basic microcavity mode electric field magnitude $|E_0(r)|$ (in decibels), corresponding to a local defect obtained by removing the shaded post in Fig. 1(b).

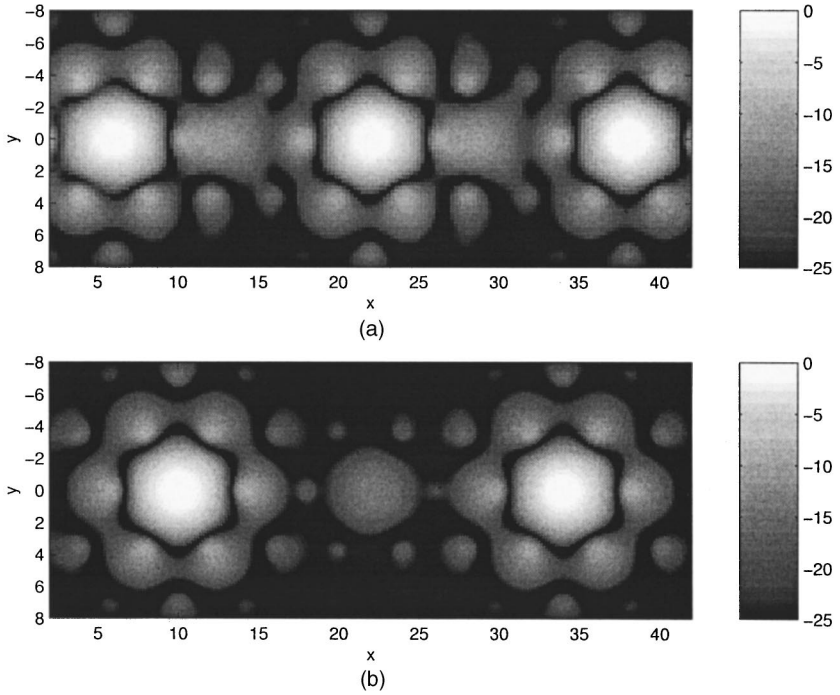

Fig. 5. Electric field magnitude in the microcavity array waveguides (in decibels): (a) $(m_1, m_2) = (2, 0)$; (b) $(m_1, m_2) = (3, 0)$.

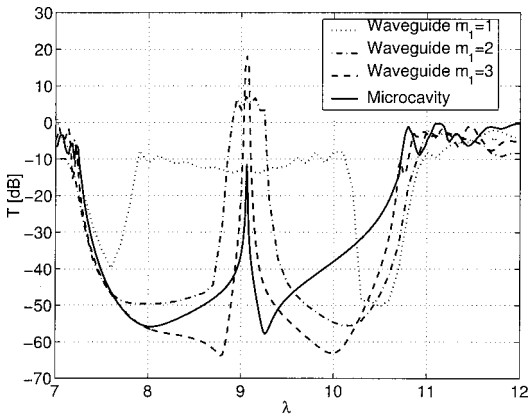

Fig. 6. Waveguide transmission curves for $m_2 = 0$ and various values of m_1 and the microcavity resonance.

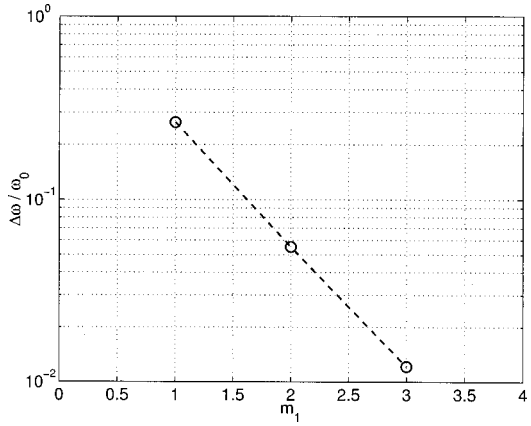

Fig. 7. Computed transmission bandwidth for $m_2 = 0$ and three values of m_1.

of shifted single-cavity modal fields that forms the basis of our study [see Eq. (2.9)]. The mismatch between the propagation properties of the waveguides and free space results in high reflection coefficients at the interfaces between the photonic crystal waveguide and free space. Consequently, both forward- and backward-propagating modes are excited in the waveguide. An uneven excitation of the cavities in Fig. 5 apparently results from interference between these forward- and backward-propagating modes. In Fig. 6 the ratio of the fields in the last and the first cavities is plotted versus wavelength. While this ratio is not the commonly used measure of transmission (transmission coefficient) for the forward propagating wave, it still allows us to identify the *true* bandwidth of the waveguide, since the cutoff frequencies are the same for forward and backward propagation. The line spectrum of a single microcavity, which defines the frequency ω_0, is shown by a solid curve. This curve represents the field in the center of a single microcavity embedded in a large (12 × 13 posts) photonic crystal, illuminated by a unit amplitude plane wave. Relation (2.21) predicts that the passband of microcavity array waveguides will be offset in frequency from the single defect resonance by a relatively small amount that is proportional to t'_{01}. Apparently the center frequency of all the waveguides considered remains very close to that of the single microcavity. Thus, t'_{01} is indeed small in all cases under study, as predicted in our theoretical analysis [see the discussion after relation (2.21)]. However, as predicted in Section 5, the bandwidth of these waveguides diminishes rapidly with increased spacing between the microcavities. We measure the bandwidth at the 20-dB points. The bandwidth dependence on $|b| = m_1|a_1|$ is depicted in Fig. 7. These results support the assertion made at the end of Section 2, namely, that the coupling between the neighboring cavities and consequently the bandwidth diminish exponentially with the intercavity spacing.

4. CONCLUSION

A novel configuration that comprises a periodic microcavity array in a photonic crystal is shown to behave as a narrow-band waveguide. The bandwidth of the waveguide can be tuned by adjusting the intercavity distances. The weak-coupling perturbation analysis that we have developed allows for analytical evaluation of the waveguiding properties. The proposed microcavity array waveguides appear to be potentially useful in the design of a variety of optical devices.

REFERENCES

1. J. D. Joannopoulos, R. D. Meade, and J. N. Winn, *Photonic Crystals: Molding the Flow of Light* (Princeton U. Press, Princeton, N.J., 1995).
2. X. P. Feng and Y. Arakawa, "Defect modes in two-dimensional triangular photonic crystals," Jpn. J. Appl. Phys. Part 2 **36**, L120–L123 (1997).
3. E. Centeno and D. Felbacq, "Guiding waves with photonic crystals," Opt. Commun. **160**, 57–60 (1999).
4. E. Centeno, B. Guizal, and D. Felbacq, "Multiplexing and demultiplexing with photonic crystals," Pure Appl. Opt. **1**, L10–L13 (1999).
5. G. Tayeb and D. Maystre, "Rigorous theoretical study of finite-size two-dimensional photonic crystals doped by microcavities," J. Opt. Soc. Am. A **14**, 3323–3332 (1997).
6. A. Boag, M. Gafni, and B. Z. Steinberg, "Bandwidth control for photonic bandgap waveguides," presented at Bianisotropics 2000, the 8th International Conference on Electromagnetics of Complex Media, Lisbon, September 27–29, 2000.
7. R. E. Peierls, *Quantum Theory of Solids* (Clarendon, Oxford, UK, 1955).
8. A. Yariv, Y. Xu, R. K. Lee, and A. Scherer, "Coupled-resonator optical waveguide: a proposal and analysis," Opt. Lett. **24**, 711–713 (1999).
9. Y. Leviatan and A. Boag, "Analysis of electromagnetic scattering from dielectric cylinders using a multifilament current model," IEEE Trans. Antennas Propag. **35**, 1119–1127 (1987).
10. A. Boag, Y. Leviatan, and A. Boag, "Analysis of two-dimensional electromagnetic scattering from a periodic grating of cylinders using a hybrid current model," Radio Sci. **23**, 612–624 (1988).